Environ. Sci. Technol. **2005**, *39,* 8653−8663

Measurements of Particle Number and Mass Concentrations and Size Distributions in a Tunnel Environment

MICHAEL D. GELLER,
SATYA BRATA SARDAR,
HARISH PHULERIA,
PHILIP M. FINE, AND
CONSTANTINOS SIOUTAS*

Department of Civil and Environmental Engineering, University of Southern California, 3620 South Vermont Avenue, Los Angeles, California 90089

Particulate matter emissions were measured in two bores of the Caldecott Tunnel in Northern California during August and September 2004. One bore (Bore 1) is open to both heavy- and light-duty vehicles while heavy-duty vehicles are prohibited from entering the second bore (Bore 2). Particulate matter number and mass size distributions, chemical composition, and gaseous copollutants were recorded for four consecutive days near the entrance and exit of each bore. Size-resolved emission factors were determined for particle number, particle mass, elemental carbon, organic carbon (OC), sulfate, nitrate, and selected elements. The size distributions in both the bores showed a single large mode at roughly 15−20 nm in mobility diameter, with occasional smaller modes around 100 nm. The PM_{10} mass emission factor for heavy-duty vehicles was 14.5 times higher than that of light-duty vehicles. The particles derived from diesel are more abundant in elemental carbon, 70.9% of PM_{10} emissions, as compared to the light-duty vehicles. Conversely, a greater percentage of OC was found in light-duty emissions than heavy-duty emissions. In comparison to previous studies at the Caldecott Tunnel, less particle mass but more particle numbers are emitted by vehicles than was the case 7 years ago.

1. Introduction

Since the U. S. Environmental Protection Agency established air pollutant standards for PM_{10} and more recently $PM_{2.5}$, particulate matter (PM) emissions from both stationary (i.e., power plants) and mobile (i.e., vehicles) sources have been significantly curtailed (*1*). These regulations were based on a multitude of both epidemiological and toxicological research that has demonstrated adverse health endpoints due to exposure to airborne particulate matter (*2*−*5*). Furthermore, because of its known carcinogenicity, the California Air Resources Board (CARB) has specifically deemed particulate matter in diesel exhaust to be a toxic air contaminant (*6*). Recent studies, however, attribute greater adverse health effects on a per mass basis to ultrafine PM (particles with d_p < 100, 150, or 180 nm, depending on the study) (*7*−*9*). Vehicular emissions have a particularly high ultrafine PM component and have been associated with an increase in cardiovascular events, respiratory symptoms, and mortality (*10*−*11*).

Vehicles constitute a major source of PM due to both direct emissions, via combustion and mechanical wear, and secondary formation, whereby organic and inorganic vapors undergo gas-to-particle conversion in the atmosphere (*12*−*13*). In the Los Angeles Basin, the dominant sources of $PM_{2.5}$ (particles with d_p < 2.5 μm) are motor vehicles (*13*). On the basis of emissions inventory estimates for 1995, it has been suggested that as much as 75% of the PM emitted from vehicles in California came from heavy-duty diesel vehicles (HDVs) (*6*). Since that time many technological advances in diesel emission controls have been implemented. One hypothesis currently gaining momentum is that while these technologies reduce particle mass emissions, they may also promote particle nucleation posttreatment, leading to a greater number of particles emitted (*14*−*15*). It should be noted that both HDVs and light-duty vehicles (LDVs, predominantly gasoline-fueled) are already known to emit high numbers of ultrafine particles (*16*), with near-roadway concentrations reaching well over 10 times urban background levels (*17*).

Many studies have measured the emissions of gaseous and particulate emissions from different vehicles. A limitation in using these results to estimate human exposure is the difference between what exits the tailpipe and what enters the respiratory tract. Various dynamometer experiments have characterized various gasoline and diesel vehicle emissions under different driving cycles and loads (*16*, *18*). Likewise, ambient PM profiles are well characterized in many locales around the world (*19*). Tunnel studies have been conducted as an intermediate between the two (*20*−*23*), getting closer to ambient conditions than a dynamometer test while allowing for average emissions measurements over a large number of vehicles. But a limitation of such studies is that tunnel conditions can vary from the ambient environment, since pollutant levels are many times greater in a tunnel. Atmospheric transformations, for instance, due to sunlight or dilution, may be limited inside of a tunnel. Particle nucleation processes may be promoted by the higher concentrations of gas-phase pollutants or limited by the increased particle surface areas found in a tunnel. In any case, tunnel sampling better approaches real-world conditions than dynamometer testing using artificial dilution systems.

The Caldecott Tunnel at Berkeley, CA, is unique in that it has one gasoline-only traffic bore and two mixed-fuel traffic bores. Two studies were conducted in 1997 to apportion various constituents of PM to either diesel or gasoline vehicles (*20*−*21*). These studies found that diesel fuel vehicles emitted much higher quantities of fine particle, black carbon, and sulfate mass per unit mass of fuel consumed compared to light-duty vehicles. Since 1997, vehicular emissions have changed for three reasons: older, high-emitting vehicles are being phased out, emissions controls on diesel engines have advanced (*24*), and fuel efficiency has increased.

The goal of this study is to provide more detailed information on number-based particle emission factors for different PM size ranges and for different vehicle types, while determining any changes in HDV and LDV emission factors since 1997. It should be noted that the present study was part of a larger, continuing effort by investigators of the Southern California Particle Center and Supersite to determine and compare the toxicity of PM emitted from HDVs and LDVs. The 1997 study conducted at this location and in

* Corresponding author phone (213)740-6134; fax(213)744-1426; e-mail: sioutas@usc.edu.

10.1021/es050360s CCC: $30.25
Published on Web 10/11/2005

TABLE 1. Traffic Volume (Vehicles h^{-1}) in Bores 1 and 2 of the Caldecott Tunnel

date	3+ axles	2-axle, 6-tire	2-axle, 4-tire	% heavy-duty diesel
Bore 2 (1200−1800 h)				
8/23/2004 (Mon)	1	29	4041	0.38
8/24/2004 (Tue)	3	38	4113	0.54
8/25/2004 (Wed)	0	20	3982	0.25
8/26/2004 (Thu)	0	28	4028	0.34
Bore 1 (1200−1800 h)				
8/30/2004 (Mon)	49	102	3013	3.2
8/31/2004 (Tue)	76	109	2482	4.9
9/1/2004 (Wed)	65	88	2951	3.5
9/2/2004 (Thu)	66	66	2741	3.4

a similar season provided us with a unique opportunity to determine trends in HDV and LDV emission factors and obtain an estimate of the effect of control strategies for PM from mobile sources over the past 7 years.

2. Methods

Airborne particle measurements inside of a roadway tunnel offer the opportunity to determine size-fractionated emission factors for particle number and different particulate chemical species. The Caldecott Tunnel connects Orinda, CA, and Berkeley, CA, along State Route 24 about 15 miles east of San Francisco. The 1.1-km-long tunnel includes three two-lane bores with a 4.2% incline from west to east (*21*). Large fans force air through ventilation shafts that span the lengths of the tunnel bores but are only activated when monitored CO levels in the tunnel reach dangerous levels. To avoid sporadic fan operation and its effects on tunnel dilution rates, the fans were disabled during the sampling period. Without the fans in operation, the motion of the vehicles caused consistently observable air flow in the direction of traffic. Direct measurements of the air flow were not necessary because the CO_2 measurements and emission factor calculations described below account for the dilution rate. Bores 1 and 3 allow both light-duty vehicles (LDVs) and heavy-duty vehicles (HDVs). Traffic flows from west to east in Bore 1. Bore 2 is restricted to LDV traffic only, and the direction of traffic switches from westward in the morning to eastward from approximately noon through the evening hours. Field sampling was conducted in Bores 1 and 2 for 4 days each (Monday through Thursday). The sampling time was from 1200 to 1800 h during August/September of 2004. Thus the traffic direction was eastbound in both bores during the sampling periods. The late August/September period corresponds to almost the same months of the 1997 studies in the same tunnel bores.

Traffic data were collected by two methods that were used to create a comprehensive traffic profile for each bore. Caldecott Tunnel personnel continuously monitor tunnel conditions from the control room with video cameras and road sensors that measure both vehicle speeds and volumes. Vehicle speed was also calculated by measuring the residence time of randomly selected vehicles in the tunnel. Videotaped counts were also taken for 1 min out of every 5 min during sampling. Table 1 shows the vehicle counts broken down by axle class. Estimates of the percentage of vehicles consuming diesel fuel were calculated based on these vehicle and axle counts (*21*), combined with fleet characteristics reported in the 2002 Vehicle Inventory and Use Survey (*25*). As was the case in Kirchstetter et al. (*21*), 50% of the 2-axle/6-tire vehicles were assumed to be diesel-powered.

Both gaseous and particulate pollutant concentrations in the tunnel bores were measured with various continuous and time-integrated instruments, approximately 50 m from the tunnel exit. Pollutant levels at the entrance of the tunnel were measured with an identical set of instrumentation located 50 m from the tunnel entrance. Because this location was also inside the tunnel, it is not an ambient background sample as it includes roadway emissions from the first 50 m of the tunnel. This location was preferable to sampling outside the tunnel entrance, because "background" levels measured there would still be influenced by the heavy traffic nearby but in a less consistent manner than inside the tunnel entrance. Emission factors were calculated based on the difference in concentrations between exit and entrance samples over a known, fixed distance of roadway between sampling locations (1000 m). The instruments were located in the air ducts just above the tunnel ceiling. Copper and antistatic tubes (conductive silicone, TSI, Inc., St. Paul, MN) were extended approximately 15 cm down into the tunnel from the air duct through vents in the tunnel ceiling. Efforts were thus made to minimize the lengths of the sampling lines, which were less than 70 cm for all of the different samplers to be described in the next section. The approximate residence time was less than 1 s in the sampling lines, which corresponds to a worst-case scenario diffusion loss of less than 8% for 10 nm particles (*26*).

TABLE 2. Instruments Deployed at Both the Entrance and the Exit of the Caldecott Tunnel Bores

instrument	species sampled
Q-Trac Plus	CO and CO_2
SMPS−CPC	particle number and size distributions
MOUDI	PM mass and metals (three size ranges)
tri-mode high-volume sampler	EC, OC, sulfate, and nitrate (three size ranges)

Table 2 gives a list of the instruments used in this study and the species sampled. The continuously measured gas species included carbon monoxide (CO) and carbon dioxide (CO_2). CO/CO_2 measurements were recorded with handheld air quality monitors (Q-Trak Plus model 8554, TSI, Inc., St. Paul, MN). The Q-Traks were calibrated with gas standards provided by the manufacturer by performing zero and span checks. This was done prior to sampling in each bore. Additionally, the Q-Traks were frequently connected to zero and span gases to confirm that no drift was occurring over the course of the study. Periodically, during each week, the instruments were crosschecked with colocated Q-Traks that were present at the tunnel as part of another experiment. Particle size distributions were recorded every 180 s using a scanning mobility particle sizer (SMPS, model 3081, TSI, Inc., St. Paul, MN) and a condensation particle counter (CPC, model 3022A, TSI, Inc., St. Paul, MN). The SMPS−CPC measured particle size distributions between 7 and 270 nm, with a sample flow of 1.5 L/min and a sheath flow of 15 L/min. Particle number concentrations were determined by integrating over the particle number size distribution. Prior to deployment, side-by-side intercomparisons of both SMPS−CPC instruments yielded excellent agreement. Both CPCs were recalibrated by the manufacturer within 4 months of the sampling campaign. CPC flows were measured and confirmed externally with calibrated rotameters.

Two instruments collected time-integrated PM_{10} samples for each 6 h sampling day. Two micro-orifice uniform deposit impactors (MOUDI, MSP, Inc., Minneapolis, MN) sampled concurrently at 30 L/min at both ends of the tunnel. Polytetrafluoroethylene (PTFE) filters (4.7 cm) were used as impaction substrates for coarse ($PM_{10}-PM_{2.5}$) and accumulation ($PM_{2.5}-PM_{0.18}$) mode PM, and a 3.7 cm PTFE after-filter was used to collect ultrafine PM ($PM_{0.18}$), in this case defined with an upper size cut of 180 nm. Two trimode

TABLE 3. Average Properties of Diesel and Gasoline Fuel

parameter	fuel type	
	diesel	gasoline
carbon weight fraction, W_c	0.87	0.85
density (g/L)	840	740
sulfur (ppm by weight)	135	12
fuel consumption (L/100 km)	47	12

high-volume impactors (*27*) sampling at 450 L/min collected the same size fractions of PM. Coarse PM was collected on a 4.7 cm quartz impaction substrate. Accumulation mode PM was collected on 10 quartz impaction strips, and ultrafine PM was collected on a 20.3 cm × 25.4 cm quartz after-filter.

Quartz filters and substrates were prebaked at 550 °C for 8 h and stored in baked aluminum-foil-lined containers prior to deployment. The MOUDI Teflon filters were analyzed for mass and trace elements. Mass concentrations were determined gravimetrically by triplicate measurements of filter weights pre- and postsampling after equilibration in a temperature (21−24 °C) and relative humidity (40−50%) controlled room. Trace elements (Pb, Ba, Cu, Fe, Mn, V, Ti, Ca, Si, Al, Mg, and Na) were measured by X-ray fluorescence (*28*). Elemental and organic carbon (EC/OC) analysis and inorganic ion analysis were performed on the quartz substrates. EC/OC concentrations were measured by thermal optical transmittance (*29*), and inorganic ion concentrations (sulfate and nitrate) were determined by ion chromatography (*30*). In most cases, the results of the chemical analyses are presented in their measured form, without adjustments or assumptions accounting for associated oxides, cations, or the hydrogen and oxygen atoms in organic compounds. The one exception is the figure attempting a mass balance (Figure 4), and the description of the adjustments are given in the Results and Discussion section below.

Emission factors were computed as described by Kirchstetter et al. (*21*), where the details on the calculations can be found. In this method, the emissions are apportioned between diesel and gasoline vehicles in the mixed bore by using the data from the gasoline bore. Emission factors are expressed in terms of mass or number emitted per kilogram of fuel burned using the CO_2 and CO measurements to determine fuel consumption. The properties of both diesel and gasoline fuels (carbon weight fraction, density, fuel consumption, and sulfur content) used for these calculations are given in Table 3 (*21*). It was assumed that the fuel bulk properties have not changed appreciably since 1997, given that the major components of the fuels have not changed. Fuel consumption (efficiency) has probably changed, but to improve comparability between the studies and due to the lack of more recent data using similar methodologies, the 1997 data was retained.

3. Results and Discussion

3.1. Traffic Characterization. Table 1 summarizes the volumes and types of vehicles in each bore for each sampling day. Although Bore 2 is essentially restricted to gasoline traffic, some medium-duty diesels and an occasional heavy-duty 3-axle vehicle passed through. As a percentage of the total vehicles counts, diesel vehicles are an order of magnitude less prevalent in Bore 2. On average, heavy-duty vehicles comprised 3.8% of vehicles in Bore 1 and less than 0.4% of vehicles in Bore 2. Total vehicle numbers were 2950 ± 220 and 4070 ± 64 in Bores 1 and 2, respectively. The number of vehicles in Bore 2 is very similar to the 1997 studies, while Bore 1 numbers have increased 25−50% above 1997 values (*20*, *21*). It should be noted that the total number of vehicles passing through the tunnel per hour nearly doubles between 1200 and 1800 h, but heavy-duty vehicles were more frequent between 1200 and 1500 h.

3.2. Pollutant Concentrations. The concentrations (after subtracting tunnel entrance levels) of CO, CO_2, PM_{10}, particle number (PN), EC, OC, sulfate, and nitrate are presented in Table 4. Concentrations of CO are comparable in both bores. This is a striking divergence from both 1997 studies, which reported roughly 50% higher CO concentrations in Bore 2 than Bore 1. This is also true of CO_2 concentrations, which were reported as roughly 75% higher in Bore 2 than Bore 1 in 1997 (*20*, *21*) but here are found to be slightly higher in Bore 1. Two likely reasons for the narrowing of the disparities between these two gaseous pollutants are: (1) total vehicle counts in Bore 1 were between 50% and 60% of those in Bore 2 in 1997 while nearly 75% in 2004 and (2) the average fuel efficiency has increased since 1997, which would cause larger reductions in CO and CO_2 in Bore 2. In contrast, HDV source apportionment of CO and CO_2 by this study compares favorably to Kirchstetter et al. (*21*), who stated that HDVs are responsible for 17% of CO_2 and 4.2% of CO emissions in Bore 1. The current study found HDV contributions of 13% of CO_2 and 3.7% of CO to total Bore 1 levels. Figures 1a and 1b show the variation of the averaged CO and CO_2 concentrations during the sampling interval. These emitted gases behave somewhat alike irrespective of the bore, with more variability present in Bore 1, which is attributable to the possibly greater heterogeneity of vehicle classes.

Since the high-volume PM samples were collected on quartz filters, they are subject to positive organic vapor adsorption artifacts that would not occur on the corresponding Teflon MOUDI substrates (*31*). Such artifacts were observed in the Caldecott Tunnel in prior studies (*20*, *21*). For this reason, the sum of individual species is greater than the gravimetrically measured mass in all samples collected in this study. The mass overbalance was observed to be much larger for the larger surface area of the ultrafine quartz filter (20.3 cm × 25.4 cm). Although it is not possible to quantify the adsorption OC artifact in this study, the ultrafine OC mass is still included in the summed PM_{10} results reported in Table 4.

PM_{10} concentrations in Bore 1 were on average 2.3 times greater than those in Bore 2. Elemental carbon constituted about 44% and 74% of PM_{10} mass in Bores 2 and 1, respectively, but actual measured concentrations were 4 times higher in Bore 1. While sulfate made up a similar percentage of PM_{10} mass in both bores (6−7%), the actual concentrations of sulfate were 2.5 times higher in Bore 1 than Bore 2. Nitrate concentrations were similar in both bores, but nitrate was 1.5% and 4% of PM_{10} mass in Bores 1 and 2, respectively. These results confirm the expected result that heavy-duty diesel vehicles, with a larger presence in Bore 1, emit more PM_{10} mass, EC, and sulfate than gasoline-powered vehicles.

While the mass concentrations were much higher in Bore 1 than Bore 2, particle number concentrations were only 25% higher in Bore 1. This result contrasts with the results of Kirchstetter et al. (*21*), who found Bore 1 concentrations to be nearly double those in Bore 2. Some possible explanations for this discrepancy will be discussed in a following section below. The similarity of average particle number concentrations in both bores can be misleading if one does not take into account the differences in traffic flow between the two bores. Bore 1, on average, has only 75% the vehicle flow of Bore 2, but higher particle number concentrations. This can be explained by the greater prevalence of heavy-duty vehicles in Bore 1, which offsets the higher vehicle counts in Bore 2. Further detail on emission factors will be discussed in a following section.

Figure 1c displays the temporal variability of PN concentrations during the sampling time interval. The figure reveals that Bore 1 PN concentrations were indeed higher

TABLE 4. Pollutant Concentrations Measured in the Caldecott Tunnel

bore and sampling time	date	average CO (ppm)	average CO_2 (ppm)	PM_{10} mass ($\mu g/m^3$)	PM_{10} EC ($\mu g/m^3$)	PM_{10} OC[a] ($\mu g/m^3$)	PM_{10} SO_4^{2-} ($\mu g/m^3$)	PM_{10} NO_3^- ($\mu g/m^3$)	average particle numbers (particles/cm^3)
Bore 2 (1200−1800 h) (gasoline only)	8/23/2004	10.5	413	14.9	8.2	14.0	0.36	0.71	5.5×10^5
	8/24/2004	9.2	352	18.9	6.0	22.9	1.22	0.11	6.9×10^5
	8/25/2004	10.1	418	15.8	6.7	32.8	1.33	0.53	1.4×10^5
	8/26/2004	9.4	359	14.4	6.9	23.2	0.94	1.15	6.7×10^5
Bore 1 (1200−1800 h) (diesel + gasoline)	8/30/2004	8.4	477	34.4	20.5	12.2	1.69	0.59	6.4×10^5
	8/31/2004	7.4	527	36.2	29.1	9.9	3.65	0.62	3.9×10^5
	9/1/2005	9.4	499	37.2	28.2	15.4	2.84	0.55	7.4×10^5
	9/2/2005	9.9	498	41.1	33.4	17.6	1.91	0.52	7.8×10^5

[a] PM_{10} mass overbalances are due to the substantial organic adosption artifact on the ultrafine quartz filter.

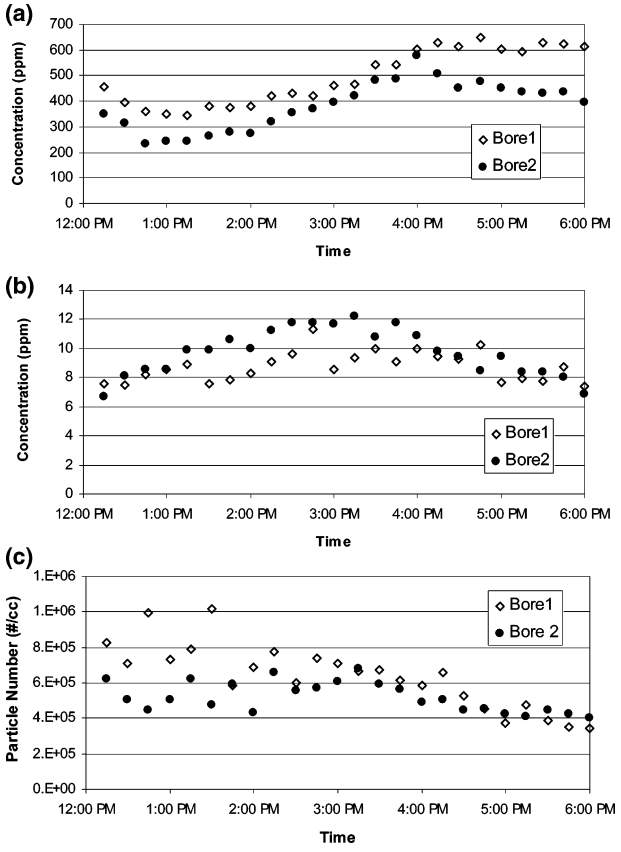

FIGURE 1. Temporal variability of gaseous and PN concentrations (averaged) in Bores 1 and 2 of the Caldecott Tunnel: (a) CO_2, (b) CO, and (c) PN.

than those in Bore 2 between 1200 and 1500 h, while number concentrations were comparable in the two bores from 1500 to 1800 h. Most of the diesel traffic in Bore 1 occurred from 1200 to 1500 h. Thus, when the data are observed over shorter time intervals, this study agrees with Kirchstetter et al. (*21*) in that even a small percentage rise in diesel vehicles does noticeably increase measured PN concentrations. Another anticipated result is the moderate correlation between CO and PN, especially in Bore 2 ($R^2 = 0.61$).

Particle number size distributions are presented in Figures 2a and 2b for Bores 1 and 2, respectively. The distributions shown are a grand average, calculated by averaging nearly 500 distributions recorded in each bore. Due to the number of scans and low frequency of diesel traffic, the average size distributions were very similar in both bores, characterized by a single mode at roughly 15−20 nm. Note that particles below 15 nm may not be efficiently measured with the current SMPS configuration due to potential diffusion losses and reduced counting efficiencies of the CPCs. Both average size distributions have sharp peaks with between 80% and 85% of particles less than 40 nm in mobility diameter. This observed trend agrees with previous studies, where size distributions from vehicular emissions were shown to have a nuclei mode peak diameter between 16 and 17 nm (*32*, *33*). The presence of such a nuclei mode has been attributed to the condensation of mostly organic species, originating in either the fuel or lube oil, onto solid nuclei such as sulfuric acid, soot, and possibly metals (*34*, *35*). Previous studies show the size of particles formed by the above-mentioned processes to be in the range of 5−50 nm (*36*, *37*).

Additionally, some individual size distributions were selected to investigate transient events in the tunnel. Occasionally (around 15% of the total sample number) a submode in the particle size distribution was observed around 60 nm in both bores (Figure 2c). This mode has been attributed to primary exhaust particles (mostly carbonaceous fractal agglomerates) originating from fuel combustion or the transformational growth of smaller particles by coagulation and vapor condensation (*38*). Kittelson et al. (*39*) have measured on-road size distributions obtained via mobile laboratory chase experiments. In terms of the relative shapes and sizes of the nucleation and accumulation modes, the on-road results of the Kittelson study are similar to the size distributions measured at the Caldecott Tunnel. The nucleation mode observed by Kittelson et al. (*39*) peaked in the 10−20 nm diameter range, and the accumulation mode at nearly 100 nm. Bore 1 displayed unique behavior in that, on few occasions, a second mode was present around 26 nm (Figure 2d). Another pattern exclusively found in Bore 1 was a much wider size distribution at certain times. Both of these phenomena may be attributable to the mixing and aging of diesel vehicle plumes within the tunnel or the variability of diesel engine types, loads, and controls.

Vehicles in the tunnel operate under various load conditions, and thus, pollutant concentrations may be related to traffic parameters such as vehicle speed. Figure 3 displays PN plotted versus vehicle speed in Bore 1. Vehicle speed was normalized by the number of vehicles, thus removing the effect of more traffic leading to higher PN. Figure 3 illustrates that PN is well correlated with normalized vehicle speed in Bore 1 ($R^2 = 0.69$). It should be noted that a moderate correlation exists between PN and vehicle speed even without normalization ($R^2 = 0.53$). Previous studies conducted by Gidhagen et al. (*40*) and Kristensson et al. (*41*) have observed a similar positive relationship between PN and traffic speed. Gidhagen et al. (*40*) theorized that PN would decrease with increasing speed due to the dependency of ventilation rate on vehicle speed. The actual result, however, was that even with more mixing and higher air exchanges in the tunnel, PN still increases with speed. This is further corroborated by a Ford Motor Co. study (*42*, *43*), which described PN emissions from light-duty vehicles traveling at higher speeds (~65 mph) to be several times higher than those emitted at lower speeds.

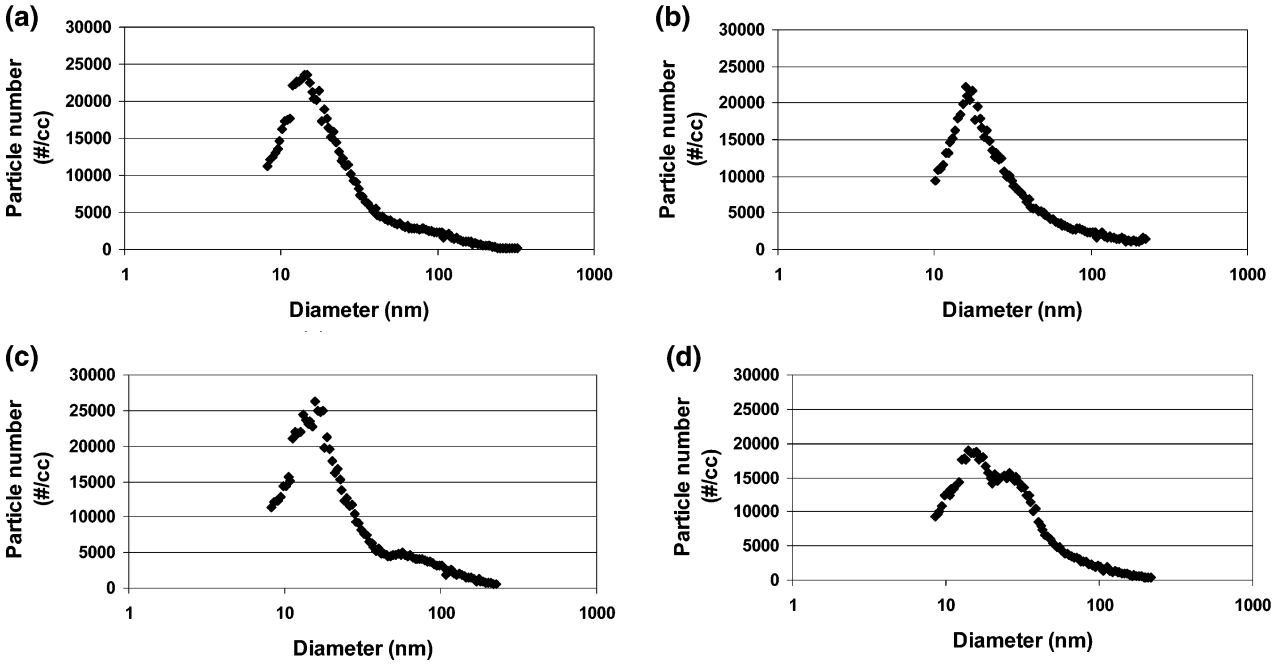

FIGURE 2. Size distributions in the Caldecott Tunnel: (a) Bore 1, (b) Bore 2, (c) snapshot showing a mode at 60 nm in Bore 1, and (d) snapshot showing a second mode (around 26 nm) in Bore 1.

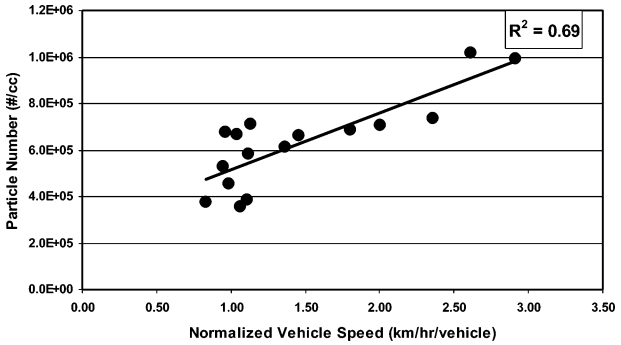

FIGURE 3. Correlation of PN vs normalized vehicle speed in Bore 1 of the Caldecott Tunnel.

3.3. Size-Resolved Chemical Composition. By examination of the size-resolved aerosol chemical composition, the sources of each chemical component can be better understood. Figures 4a, 4b, and 4c provide the concentrations of major chemical species measured in Bores 1 and 2 for coarse (2.5−10 μm), accumulation (0.18−2.5 μm), and ultrafine (0−0.18 μm) modes, respectively. For the purposes of this figure and mass balance considerations, measured species were adjusted to account for associated atoms. Nitrate and sulfate were assumed to exist as ammonium nitrate and ammonium sulfate, trace elements were assumed to exit in their most common oxide form, and OC was converted to organic mass (OM) using a factor of 1.4 (*44*). All concentrations were obtained by subtracting the tunnel entrance concentration from the exit concentration. The horizontal lines intersecting the bars in Figures 4a−c represent the gravimetric mass measured by the MOUDI for the respective size fraction. In every case, the sum of the chemical species is larger than the weighed mass, which could be due either to errors in the assumptions of associated atoms or to organic adsorption artifacts. Since vapor adsorption is favored during filtration over impaction, the discrepancies between reconstructed mass and gravimetric mass are much larger in the ultrafine samples, as seen in Figure 4c. For the coarse and accumulation modes, the differences between reconstructed and measured mass concentrations are within 20% or less, an indication that adsorption artifacts may not be as important for these two size ranges.

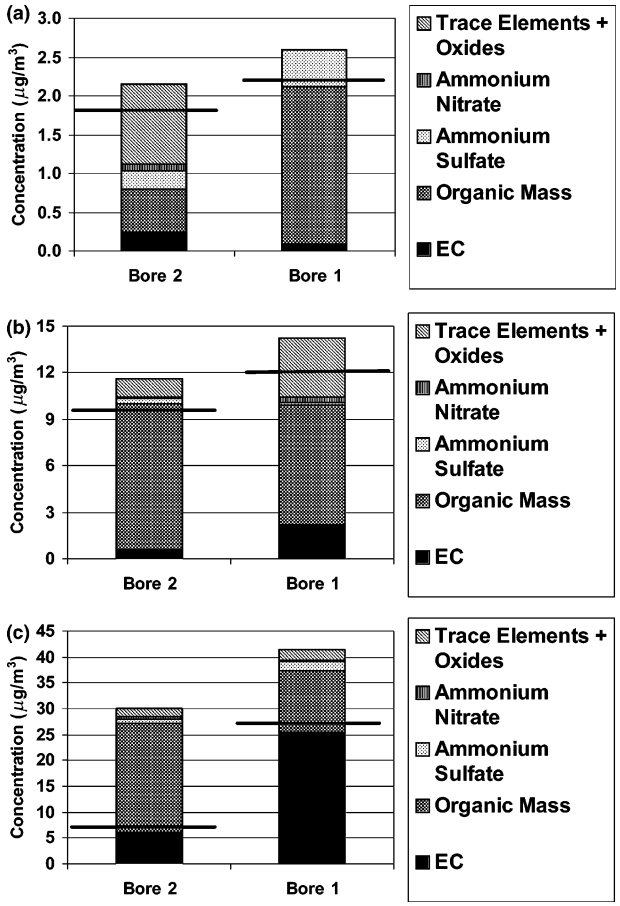

FIGURE 4. Size-resolved chemical composition in Bores 1 and 2 of the Caldecott Tunnel for (a) coarse (2.5−10 μm), (b) accumulation (0.18−2.5 μm), and (c) ultrafine (0−0.18 μm) modes. Horizontal lines represent the gravimetrically determined mass.

Figure 4a shows the coarse concentrations of chemical species in Bores 1 and 2. Trace elements and OM were the

dominant components in the coarse mode of Bore 2 with contributions of 48 ± 5% and 26 ± 6%, respectively, to the reconstructed mass. EC, ammonium sulfate, and ammonium nitrate comprised 11 ± 4%, 11 ± 2%, and 4.4 ± 1%, respectively, of the total coarse mass in Bore 2. In Bore 1, OM contributed 79 ± 24% of the coarse mass. With a higher contribution from diesel vehicles, the coarse ammonium sulfate concentration in Bore 1 is 18 ± 3% of the total. Coarse sulfate in Bore 1 possibly comes from resuspended road dust, which may include sulfates from the long-term deposition of emitted smaller particles and/or oil and water drippings to the roadway. EC constituted 3.4 ± 1.1% of Bore 1 coarse PM while trace elements and ammonium nitrate were below tunnel entrance levels. The absence of trace elements from Bore 1 coarse PM was somewhat unexpected and will be discussed further below.

$PM_{2.5}$ mass accounted for more than 90% of the PM_{10} mass in Bore 2 and nearly 95% of PM_{10} in Bore 1. The accumulation mode in both bores was dominated by organic compound mass contributing 81 ± 16% and 54 ± 6% to the total mass in Bores 2 and 1, respectively. EC was only 5.1 ± 1.4% of Bore 2 accumulation mode PM mass with a concentration of 0.6 ± 0.12 $\mu g/m^3$. The concentration of accumulation mode EC in Bore 1 was 2 ± 1.0 $\mu g/m^3$ or 16 ± 4% of the total accumulation mode mass. Studies have shown that diesel vehicles are larger emitters of EC as compared to gasoline-fueled vehicles (*20*, *21*).

Figure 4c represents the chemical composition of the ultrafine mode in Bores 1 and 2. Note that the OM concentrations shown may be substantially overestimated due to positive artifacts related to the adsorption of gas-phase species on the quartz fiber filters, a well-known phenomenon when collecting PM for organic analysis using quartz filters (*45*−*47*). Depending upon the selection of the split point in the EC/OC analysis, it is possible that higher OC loadings may lead to larger errors in the EC concentrations. Regardless of the sampling error, the relative proportions of EC and OC shown in Figure 4c agree with prior research. The concentration of EC was over 4 times higher in Bore 1 than that in Bore 2, and it made up over 50% of Bore 1 ultrafine mass.

In addition to EC, the sulfate emissions in Bore 1 were also observed to be higher than those in Bore 2 (coarse and ultrafine modes). A number of studies have associated higher sulfate emissions to heavy-duty vehicles, and the observed higher concentrations in Bore 1 are most likely due to the higher percentage of heavy-duty vehicles in Bore 1 (*20*, *21*). The PM_{10} sulfate concentrations in Bores 1 and 2 of this study were 2.5 and 0.96 $\mu g/m^3$, respectively, similar to the results of Kirchstetter et al. (2.17 and 0.82 $\mu g/m^3$ in Bores 1 and 2, respectively) (*21*). Although the levels of sulfur in diesel fuel have been decreasing over the past few decades, the present California maximum sulfur content of 500 ppm by weight in diesel fuel has been in force since 1993 (*6*). A new regulation is expected to take effect in 2006, at which time the maximum sulfur content in diesel fuel will be reduced to 15 ppm by weight (*6*). Future tunnel studies may substantiate the reduction of sulfate emissions from diesel vehicles due to the lower sulfur content of diesel fuel.

Besides particulate EC and OC, road traffic is recognized to be an important source of particulate metal and other trace element emissions (*48*−*53*). A number of these metals have been associated with toxic properties (*54*−*55*). On-road sources of particle-bound metals and trace elements include: combustion products from fuel additives/impurities, abrasion of brake linings, tire wear, and the resuspension of road dust. The size-resolved trace element concentrations at the exits and entrances of Bores 2 and 1 are shown in Figures 5 and 6, respectively. Figures 5a−c display the concentrations of selected trace elements in Bore 2 for the

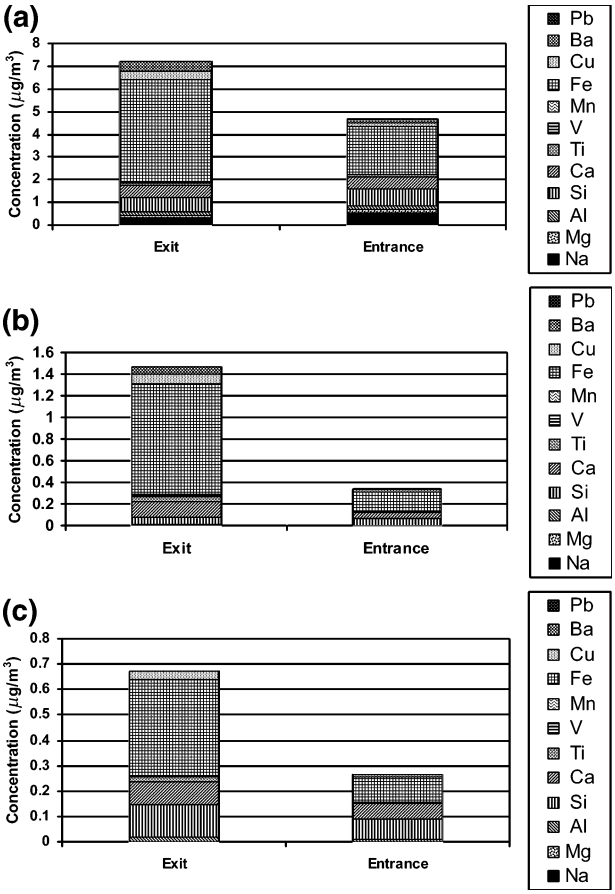

FIGURE 5. Size-resolved trace element concentrations measured at the entrance and exit of Bore 2 for (a) coarse (2.5−10 μm), (b) accumulation (0.18−2.5 μm), and (c) ultrafine modes (0−0.18 μm).

coarse, accumulation, and ultrafine modes, respectively. The measured elemental concentrations at the exit of Bore 2 were found to be higher than those at the entrance for all three size fractions. The tunnel exit-to-entrance ratios of total trace element concentrations in Bore 2 are 1.5, 4.4, and 2.5 for the coarse, accumulation, and ultrafine modes, respectively. Nearly 77% of the total PM_{10} trace element concentration at the tunnel exit was from the coarse mode, while the ultrafine fraction contributed only 7%. Iron (Fe) dominated all three modes inside the tunnel, with higher levels observed at the exit than the entrance. Some of the Fe emitted (especially in the coarse mode) can be explained by contributions from resuspension of earth or geologic materials from the roadway, but the observed levels in the smaller size fractions are indicative of a nongeologic source. Another potential source of Fe includes particles exiting tail pipes from engine wear as well as brake wear (*56*). A study by Singh et al. (*57*) reported size distributions and diurnal characteristics of particle-bound metals at a traffic-dominated site versus a more rural location. This and other studies have shown higher fine particle-bound Fe concentrations at near-traffic sites, indicating an association between Fe emissions and vehicular traffic (*58*).

A closer look at Figures 5a and 5b reveals that in the coarse and accumulation mode, the Al-to-Si ratios were identical at both the entrance and the exit of Bore 2. This consistency is an indication that soil dust was resuspended at both the entrance and the exit of the bore (*12*, *59*, *60*). The Al-to-Si ratio was not consistent for the ultrafine mode because ultrafine particle-bound silicon is thought to be of vehicular origin (*59*). Sanders et al. (*56*) has reported that silicon is present in the rotors of vehicles and silica is sometimes present in brake linings of vehicles as an abrasive. Garg et

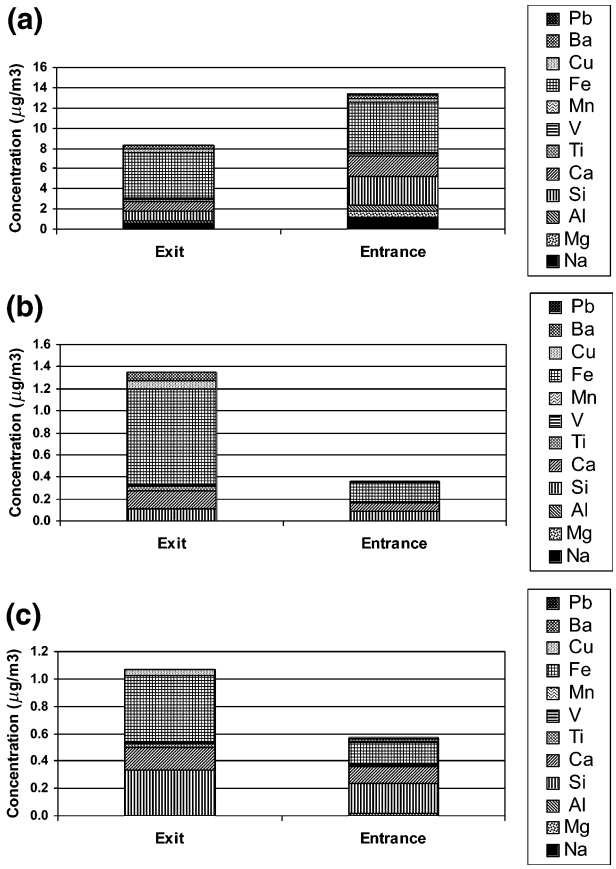

FIGURE 6. Size-resolved trace element concentrations measured at the entrance and exit of Bore 1 for (a) coarse (2.5−10 μm), (b) accumulation (0.18−2.5 μm), and (c) ultrafine modes (0−0.18 μm).

al. (*61*) showed that the high temperatures at the brake/rotor interface are hot enough to melt and decompose brake lining materials and produce ultrafine emissions. Silicon has also been observed in ultrafine ambient samples (*62*) as well as in fine particle tailpipe emission from vehicles (*59*). Higher concentrations of Ti and Cu in all three PM size fractions and higher Ba concentrations in the coarse and accumulation modes were observed at the Bore 2 exit. A study by Sternbeck et al. (*63*) has found brake linings to be a major source of Cu (used as a high-temperature lubricant), Ba, and Pb. Sanders et al. (*56*) reported that airborne wear debris from automobile brakes tested in both dynamometer and test track driving experiments contains Ti, Cu, and Ba. The present elemental analysis shows enriched Fe, Cu, and Ba concentrations in the tunnel, which is consistent with the brake dust fingerprint reported by Sternbeck et al. (*63*).

Furthermore, Figures 5b and 5c reveal that Bore 2 accumulation and ultrafine Ca concentrations were also elevated at the tunnel exit when compared to the entrance. The source of Ca in the fine fraction ($PM_{2.5}$) can possibly be traced to the use of calcium soaps in automotive lubricating oils (*64*). Singh et al. (*57*) have also shown a significant proportion of calcium in the submicron (0.35−1.0 μm) particles at a traffic-dominated site in the Los Angeles Basin. The comparable levels of Ca in both ends of Bore 2 in the coarse size fraction (0.49 and 0.56 $\mu g/m^3$ at the exit and entrance of the tunnel, respectively) most likely point to crustal material as a common source.

Figures 6a−c show the size-resolved trace element concentrations at the entrance and exit of Bore 1. An interesting result in Figure 6a is the decrease in coarse mode trace elements between the bore entrance and the exit. The tunnel thus appears to be a "sink" rather than a source of coarse particle trace elements, even though the Bore 1 coarse mass, EC, OC, and sulfate concentrations increased from entrance to exit. Bore 2 coarse trace elements did not exhibit the same behavior. Examination of the ratios of tunnel exit to tunnel entrance trace element concentrations for all three size modes in both bores yields a clearer picture. Those elements with only crustal sources in the coarse mode (Al, Si, Ca, and Mg) had average exit-to-entrance ratios (± standard deviation) of 0.85 ± 0.08 and 0.35 ± 0.05 in Bores 2 and 1, respectively. Moreover, the average ratios of the three common brake dust elements (Fe, Cu, and Ba) were 2.5 ± 0.5 and 1.0 ± 0.1 in Bores 2 and 1, respectively. Therefore, the ratios of the exit concentrations to the entrance concentrations in Bore 1 are approximately 2.5 times smaller than those of Bore 2, irrespective of the two stated sources. Bore 2 has a reversible traffic direction, allowing westbound traffic in the mornings and eastbound traffic in the afternoons. We hypothesize that vehicles resuspend and carry coarse road dust (from both crustal and vehicular wear) into the tunnel from both sides of Bore 2, while from only the western side of Bore 1. Because vehicles are equally likely to brake at either side of the tunnel, the concentrations of elements associated with brake dust remain constant in Bore 1 at both the entrance and the exit. Bore 2 has a ratio of 2.5 because particle-bound elements from brake linings deposited at the entrance during the morning hours are being resuspended as vehicles exit the tunnel in the afternoon, which adds to the trace elements currently being emitted from the cars. Similarly, Bore 2 has a nearly 1:1 ratio of coarse crustal elemental species due to equal deposition of road dust at either side of the tunnel due to reversible traffic. Without the morning deposition, the coarse crustal elements resuspended at the entrance to Bore 1 settle out gravitationally before reaching the exit, explaining the lower levels of these crustal elements at the exit of Bore 1.

Comparing Figures 5b and 5c to Figures 6b and 6c further corroborates these points. The fine particle-bound Si, Ca, Fe, Ti, and Cu concentrations measured at the Bore 1 exit were higher than those measured at the tunnel entrance. Bore 1 and 2 accumulation mode and ultrafine mode particle-bound trace elements behaved similarly, most likely due to constant emission rates throughout the tunnel and the longer atmospheric residence times resulting from their smaller sizes. In a few cases, the ratio of an element (i.e., Si) to the total trace element mass differed between bores, which may be a result of the differences in vehicle classes.

3.4. Emission Factors. The size-segregated emission factors for PN are given in Table 5, and Table 6 provides the emission factors for PM mass, elements, and chemical species for three size modes (coarse, accumulation, and ultrafine). While heavy-duty vehicles only constituted 3.8% of total traffic in Bore 1, they were responsible for 36% of the total number of particles. In comparison to light-duty vehicles, heavy-duty diesel vehicles have higher PN emission factors for every size fraction listed in Table 5. The integrated PN emission factors for heavy-duty and light-duty vehicles were found to be 8.21×10^{15} particles per kilogram of diesel burned and 2.48×10^{15} particles per kilogram of gasoline burned, respectively. Regardless of vehicle class, emissions of particles in the 10−18 nm range were the highest, as was seen in the particle size distributions. It is interesting to note that the ratio of HDV-to-LDV emission factors increases with particle size range. For example, while HDVs emit roughly 3−4 times more particles by numbers in the 10−100 nm range, they emit 5 times more particles in the 100−180 nm range and almost 10-fold higher in the >180 nm range. This observation is consistent with the fact that HDVs have higher emissions of fractal-like soot agglomerates, many of which have mobility diameters in the accumulation mode, even though their low density places them in the ultrafine mode when aerodynamic diameter is considered (*65*).

TABLE 5. Total and Size-Resolved PN Emission Factors (Number of Particles per Kilogram of Fuel Burned) for Light-Duty Vehicles and Heavy-Duty Diesel Vehicles in the Caldecott Tunnel

day	10−18 nm	18−32 nm	32−56 nm	56−100 nm	100−180 nm	>180 nm	total
			Light-Duty Vehicles				
1	1.3×10^{15}	6.5×10^{14}	2.4×10^{14}	1.3×10^{14}	5.6×10^{13}	5.9×10^{12}	2.3×10^{15}
2	1.9×10^{15}	1.1×10^{15}	3.7×10^{14}	1.6×10^{14}	6.7×10^{13}	8.0×10^{12}	3.6×10^{15}
3	2.5×10^{14}	2.1×10^{14}	6.6×10^{13}	3.4×10^{13}	1.5×10^{13}	2.2×10^{12}	5.8×10^{14}
4	8.3×10^{14}	1.5×10^{15}	6.3×10^{14}	3.1×10^{14}	1.3×10^{14}	1.7×10^{13}	3.4×10^{15}
grand average	1.1×10^{15}	8.6×10^{14}	3.3×10^{14}	1.6×10^{14}	6.7×10^{13}	8.2×10^{12}	2.5×10^{15}
standard deviation	7.0×10^{14}	5.4×10^{14}	2.4×10^{14}	1.1×10^{14}	4.8×10^{13}	6.2×10^{12}	1.4×10^{15}
			Heavy-Duty Diesel Vehicles				
1	4.3×10^{15}	1.6×10^{15}	4.8×10^{14}	3.3×10^{14}	2.0×10^{14}	9.3×10^{13}	7.0×10^{15}
2	4.9×10^{15}	3.6×10^{15}	1.4×10^{15}	7.7×10^{14}	4.2×10^{14}	7.4×10^{13}	1.1×10^{16}
3	3.7×10^{15}	1.1×10^{15}	7.5×10^{14}	4.7×10^{14}	3.7×10^{14}	6.0×10^{13}	6.5×10^{15}
grand average	4.3×10^{15}	2.1×10^{14}	8.8×10^{14}	5.2×10^{14}	3.3×10^{14}	7.5×10^{13}	8.2×10^{15}
standard deviation	5.5×10^{14}	1.3×10^{15}	4.9×10^{14}	2.3×10^{14}	1.2×10^{14}	1.7×10^{13}	2.5×10^{15}

TABLE 6. Light-Duty Vehicle and Heavy-Duty Diesel Emission Factors (mg kg^{-1}) of Fuel Burned (average ± standard deviation)[a]

	mode		
	coarse (2.5−10 μm)	accumulation (0.18−2.5 μm)	ultrafine (<0.18 μm)
	Light-Duty		
mass	7.7 ± 1.6	40 ± 8	27.1 ± 3.2
OC	2.4 ± 0.9	7.4 ± 2.3	**
EC	1.0 ± 0.6	2.6 ± 1.2	26.8 ± 3.1
nitrate	0.6 ± 0.3	0.42 ± 0.2	1.2 ± 0.9
sulfate	0.8 ± 0.4	1.1 ± 0.9	2.7 ± 1.8
Mg	0.4 ± 0.2	0 ± 0	0 ± 0
Al	0.2 ± 0.4	0 ± 0	0.1 ± 0.1
Si	1.6 ± 1.3	0.1 ± 0.1	0.3 ± 0.1
Ca	0.8 ± 0.3	0.4 ± 0.2	0.3 ± 0.0
Fe	10.4 ± 3.1	3.7 ± 0.9	1.23 ± 0.50
Ti	0.3 ± 0.2	0.2 ± 0.1	0.1 ± 0.0
Ba	1.2 ± 0.9	0.3 ± 0.2	0 ± 0
	Heavy-Duty		
mass	75 ± 15	304 ± 62	711 ± 65
OC	12.3 ± 2.6	19.0 ± 5.6	*b*
EC	66 ± 17	306 ± 44	403 ± 32
nitrate	0.4 ± 0.0	4.5 ± 1.0	1.8 ± 0.9
sulfate	1.9 ± 0.5	10.7 ± 0.4	37 ± 9
Mg	−8.2 ± 6.3	0.0 ± 0.0	0.0 ± 0.0
Al	−12.2 ± 1.9	0.0 ± 0.0	0.6 ± 0.2
Si	−51 ± 44	0.6 ± 0.1	0.6 ± 0.3
Ca	−30 ± 9	0.3 ± 0.1	0.2 ± 0.1
Fe	−154 ± 58	4.3 ± 2.0	2.8 ± 0.9
Ti	−3.3 ± 1.7	1.3 ± 0.2	0.8 ± 0.1
Ba	−15.2 ± 3.5	0.9 ± 0.1	0.0 ± 0.0

[a] Negative values reflect the higher tunnel entrance levels relative to exit levels. [b] Not presented due to a substantial organic adsorption artifact.

The size-segregated average emission factors for each measured species are shown with their associated standard deviations in Table 6. It can be concluded from Table 6 that emissions from heavy-duty vehicles for all three size fractions are higher than those of the light-duty vehicles for most of the species sampled. The estimated mass emission factors for heavy-duty vehicle-emitted coarse, accumulation, and ultrafine PM (average ± standard deviation) are 75 ± 16, 304 ± 62, and 711 ± 65 mg/kg of fuel burned, respectively, while the corresponding emissions by light-duty vehicles are 7.7 ± 1.6, 41 ± 8, and 27 ± 3 mg/kg of fuel consumed. The PM_{10} mass emission factor for heavy-duty vehicles is 14.5 times higher than that of light-duty vehicles. Carbonaceous material comprised the majority of emissions. Particles derived from diesel are more abundant in elemental carbon (70.9% of PM_{10} emissions) than the light-duty vehicle emissions with a lower EC fraction (40.5%). Conversely, particle-bound OC constituted a greater percentage of light-duty vehicle emissions than it does for HDVs. The OC collected in the ultrafine mode may have associated adsorption artifacts, and hence the OC concentrations in this mode were not considered for emission factor calculations. HDVs emitted nearly 11 times more PM_{10} sulfate than LDVs, with the greatest disparity in the ultrafine mode (factor of ~13.5). As a percentage of PM_{10} mass, however, emissions did not differ greatly from one another. (4.5% and 6.1% of PM_{10} mass emissions from LDVs and HDVs, respectively). Both LDVs and HDVs were minor sources of particle-bound nitrate.

Table 6 also depicts the emission factors for a number of trace elements. The results show that iron has a strikingly high emission factor attributed to LDVs. The PM_{10} emission factor for Fe from light-duty vehicles is estimated to be 15.3 mg/kg of gasoline consumed. Although HDV emission factors for coarse PM trace elements appear negative due to the subtraction of entrance concentrations from exit concentrations (see above discussion), the measured trace element levels at the entrance of Bore 1 were higher than those at the entrance of Bore 2. HDV traffic has been associated with higher emissions of resuspended road dust than LDVs (*66*).

TABLE 7. Comparison of the Current Measured Concentrations of CO_2 and Emission Factors of $PM_{2.5}$ and PN to Measurements Made in Previous Studies at the Caldecott Tunnel

vehicle type	study	CO_2 (ppm)	$PM_{2.5}$ (g/kg)	particle number (particles/kg)
LDV	this work	384	0.07 ± 0.02	$(2.5 \pm 1.4) \times 10^{15}$
LDV	Kirchstetter et al. (*21*)	665	0.11 ± 0.01	$(4.6 \pm 0.7) \times 10^{14}$
LDV	Allen et al. (*20*)	738.5	0.07 ± 0.05[a]	*b*
HDV	this work	515	1.02 ± 0.04	$(8.2 \pm 2.5) \times 10^{15}$
HDV	Kirchstetter et al. (*21*)	373	2.5 ± 0.2	$(6.3 \pm 1.9) \times 10^{15}$
HDV	Allen et al. (*20*)	435.5	1.285 ± 0.2*	*b*

[a] Represents $PM_{1.9}$. [b] Not available.

3.5. Comparisons to Previous Research. Table 7 compares the CO_2 concentrations and the $PM_{2.5}$ and PN emission factors determined in this study with those from previous studies in the Caldecott Tunnel. Kirchstetter et al. (*21*) gives LDV and HDV $PM_{2.5}$ emission factors of 0.11 ± 0.01 and 2.5 ± 0.2 g kg^{-1}, respectively, while the corresponding values observed in the current 2004 study are 0.07 ± 0.02 and 1.02 ± 0.04 g kg^{-1}. LDV $PM_{2.5}$ emissions have dropped by 37%, and HDV $PM_{2.5}$ emissions have declined 60% in the past 7 years. Although Allen et al. (*20*) calculated $PM_{1.9}$ emission factors, it is worth noting that the 2004 $PM_{2.5}$ emission factors reported here are still lower than the $PM_{1.9}$ emission factors

from 1997. The CO and CO_2 concentrations are notably different as compared to 1997 values. One hypothesis is the increase in average fleet fuel efficiency due to phasing out of older, less fuel-efficient engines. This might help explain the overall decline in mass emissions as well. However, HDV PM emissions have fallen much more dramatically than can be explained by fuel efficiency alone. The 60% decrease in HDV $PM_{2.5}$ emissions may also be explained by increased use of more efficient diesel engine emissions controls, which have become more prevalent due to regulations on diesel truck emissions (*24*).

While the decline in mass-based particle emissions is a perceived success of the regulatory system, a very different trend can be observed for number-based particle emissions. Since 1997 LDV particle number emission rates have increased by a factor of 5.4 and HDVs by 1.3. This finding is of particular note considering that (1) the latest research indicates that ultrafine particles, which comprise over 95% of total particle number, induce the greatest adverse health effects (*7*, *9*, *67*) and (2) the focus of vehicle emissions regulations has moved away from LDVs and toward HDVs in the recent past.

In making comparisons of particle number emission factors between the current and the previous study (*21*), it is important to consider the different sampling configurations and the potential for differing degrees of particle losses in the sampling lines. In the previous study, a 46 m sampling line was used with a flow rate of 5.2 L/min. With the typical size distributions given in Figure 2 and assuming laminar flow, the diffusion losses in their sampling lines is calculated to be approximately 15% of the total particle number (*26*). By contrast, the losses in the current configuration are less than 4%. Thus, even though the Kirchstetter et al. (*21*) study may have slightly underestimated the total particle number by 15%, this error cannot account for the entire 30% and 540% increases in particle number emission factors for HDVs and LDVs, respectively.

There may be several explanations for the apparent increases in particle number emissions even though particle mass-based emissions decreased substantially. It is generally accepted that vehicles, especially HDVs, emit two different types of particles: carbonaceous solid particles (mostly soot), whose fractal agglomerate-like structure places them in the accumulation mode (i.e., >100 nm in mobility diameter), and more semivolatile particles, mostly found in the <50 nm range, comprising the so-called nucleation mode (*68*, *69*). Older engines emit higher concentrations of carbonaceous material, offering a large surface area for adsorption of condensable volatile compounds, a process that counteracts the formation of smaller particles by nucleation. As the emissions of carbonaceous PM of newer engines decreases, the formation of nucleation mode particles is favored due to the reduction of the available surface for adsorption of the semivolatile material. The resulting supersaturation of the mostly organic vapor increases the production of nanoparticles by nucleation (*34*, *70*). Interestingly, this effect appears to be more pronounced when particle traps are used. (*71*). Nucleation becomes especially strong if catalytic aftertreatment devices (catalytic traps or catalytic converters) are applied. For example, the oxidation of SO_2 to SO_3 leads to the formation of sulfuric acid droplets, which act as the main nucleating species onto which semivolatile organics condense to form ultrafine particles (*15*).

Although tunnels have very different characteristics than dynamometer and open freeway environments, results from those types of studies can be used to put this study's results in context. Size distributions near two Los Angeles freeways, one primarily gasoline and one diesel plus gasoline, have been reported by Zhu et al. (*17*). While the shape of the size distribution near the mixed freeway compares well to those from this study, the gasoline-only freeway size distribution is much broader than the current study with an absence of a sharp peak. On-road vehicle size distribution measurements compare favorably to the tunnel distributions reported here (*34*). In comparison to both of the above cases, the tunnel particle numbers are almost an order of magnitude higher, which may have implications for human exposure inside roadway tunnels. Dynamometer studies have reported sharp peaks very close to the mode diameters reported in this study (*71*).

Acknowledgments

The authors acknowledge Robert Harley of the University of California, Berkeley, Susanne Hering of Aerosol Dynamics, Inc., and Antonio Miguel, Arantza Eiguren, and Bill Grant of the University of California, Los Angeles. We also gratefully acknowledge the Caltrans Caldecott Tunnel crew. This research was supported by the Southern California Particle Center and Supersite, funded by the Environmental Protection Agency under the STAR program through Grant Nos. 53-4507-0482 and 53-4507-7721 to the University of Southern California. The research described in herein has not been subjected to the Agency's required peer and policy review and therefore does not necessarily reflect the views of the agency, and no official endorsement should be inferred. Mention of trade names or commercial products does not constitute an endorsement or recommendation for use.

Literature Cited

(1) U. S. EPA. *The Particle Pollution Report: Current Understanding of Air Quality and Emissions through 2003*; EPA 454-R-04-002; Monitoring and Analysis Division, Office of Air Quality Planning and Standards Emissions: Research Triangle Park, NC, 2004.

(2) Dockery, D. W.; Pope, C. A.; Xu, X. P.; Spengler, J. D.; Ware, J. H.; Fay, M. E.; Ferris, B. G.; Speizer, F. E. An association between air-pollution and mortality in 6 United-States cities. *N. Engl. J. Med.* **1993**, *329*, 1753−1759.

(3) Pope, C. A.; Dockery, D. W.; Schwartz, J. Review of epidemiological evidence of health-effects of particulate air-pollution. *Inhalation Toxicol.* **1995**, *7*, 1−18.

(4) Adler, K. B.; Fischer, B. M.; Wright, D. T.; Cohn, L. A.; Becker, S. Interactions between respiratory epithelial-cells and cytokines—Relationships to lung inflammation. *Ann. N. Y. Acad Sci.* **1994**, *725*, 128−145.

(5) Ferin, J.; Oberdorster, G.; Penney, D. P.; Soderholm, S. C.; Gelein, R.; Piper, H. C. Increased pulmonary toxicity of ultrafine particles. 1. Particle clearance, translocation, morphology. *J. Aerosol Sci.* **1990**, *21*, 381−384.

(6) Air Resources Board, Californa Environmental Protection Agency. *Fact Sheet: California Low Sulfur Diesel Fuel*; California Environmental Protection Agency: Sacramento, CA, 2003.

(7) Li, N.; Sioutas, C.; Cho, A.; Schmitz, D.; Misra, C.; Sempf, J.; Wang, M. Y.; Oberley, T.; Froines, J.; Nel, A. Ultrafine particulate pollutants induce oxidative stress and mitochondrial damage. *Environ. Health Perspect.* **2003**, *111*, 455−460.

(8) Oberdorster, G. Pulmonary effects of inhaled ultrafine particles. *Int. Arch. Occup. Environ. Health* **2001**, *74*, 1−8.

(9) Xia, T.; Korge, P.; Weiss, J. N.; Li, N.; Venkatesen, M. I.; Sioutas, C.; Nel, A. Quinones and aromatic chemical compounds in particulate matter induce mitochondrial dysfunction: Implications for ultrafine particle toxicity. *Environ. Health Perspect.* **2004**, *112*, 1347−1358.

(10) Riediker, M.; Cascio, W. E.; Griggs, T. R.; Herbst, M. C.; Bromberg, P. A.; Neas, L.; Williams, R. W.; Devlin, R. B. Particulate matter exposure in cars is associated with cardiovascular effects in healthy young men. *Am. J. Respir. Crit. Care Med.* **2004**, *169*, 934−940.

(11) Garshick, E.; Laden, F.; Hart, J. E.; Caron, A. Residence near a major road and respiratory symptoms in US veterans. *Epidemiology* **2003**, *14*, 728−736.

(12) Schauer, J. J.; Rogge, W. F.; Hildemann, L. M.; Mazurek, M. A.; Cass, G. R. Source apportionment of airborne particulate matter using organic compounds as tracers. *Atmos. Environ.* **1996**, *30*, 3837−3855.

(13) Mysliwiec, M. J.; Kleeman, M. J. Source apportionment of secondary airborne particulate matter in a polluted atmosphere. *Environ. Sci. Technol.* **2002**, *36*, 5376−5384.

(14) Sakurai, H.; Park, K.; McMurry, P. H.; Zarling, D. D.; Kittelson, D. B.; Ziemann, P. J. Size-dependent mixing characteristics of volatile and nonvolatile components in diesel exhaust aerosols. *Environ. Sci. Technol.* **2003**, *37*, 5487−5495.
(15) Vaaraslahti, K.; Virtanen, A.; Ristimaki, J.; Keskinen, J. Nucleation mode formation in heavy-duty diesel exhaust with and without a particulate filter. *Environ. Sci. Technol.* **2004**, *38*, 4884−4890.
(16) Burtscher, H. Physical characterization of particulate emissions from diesel engines: A review. *J. Aerosol Sci.* **2005**, *36* (7), 896−932.
(17) Zhu, Y. F.; Hinds, W. C.; Shen, S.; Sioutas, C. Seasonal trends of concentration and size distribution of ultrafine particles near major highways in Los Angeles. *Aerosol Sci. Technol.* **2004**, *38*, 5−13.
(18) Kleeman, M. J.; Schauer, J. J.; Cass, G. R. Size and composition distribution of fine particulate matter emitted from motor vehicles. *Environ. Sci. Technol.* **2000**, *34*, 1132−1142.
(19) Latha, K. M.; Badarinath, K. V. S. Seasonal variations of PM10 and PM2.5 particles loading over tropical urban environment. *Int. J. Environ. Health Res.* **2005**, *15*, 63−68.
(20) Allen, J. O.; Mayo, P. R.; Hughes, L. S.; Salmon, L. G.; Cass, G. R. Emissions of size-segregated aerosols from on-road vehicles in the Caldecott Tunnel. *Environ. Sci. Technol.* **2001**, *35*, 4189−4197.
(21) Kirchstetter, T. W.; Harley, R. A.; Kreisberg, N. M.; Stolzenburg, M. R.; Hering, S. V. On-road measurement of fine particle and nitrogen oxide emissions from light- and heavy-duty motor vehicles. *Atmos. Environ.* **1999**, *33*, 2955−2968.
(22) Fraser, M. P.; Cass, G. R.; Simoneit, B. R. T. Gas-phase and particle-phase organic compounds emitted from motor vehicle traffic in a Los Angeles roadway tunnel. *Environ. Sci. Technol.* **1998**, *32*, 2051−2060.
(23) Chellam, S.; Kulkarni, P.; Fraser, M. P. Emissions of organic compounds and trace metals in fine particulate matter from motor vehicles: A tunnel study in Houston, Texas. *J. Air Waste Manage. Assoc.* **2005**, *55*, 60−72.
(24) Air Resources Board, California Environmental Protection Agency. *Risk Reduction Plan to Reduce Particulate Matter Emissions from Diesel-Fueled Engines and Vehicles*; Stationary Source Division, Mobile Source Control Division, California Environmental Protection Agency: Sacramento, CA, 2000.
(25) U. S. Census Bureau. *California Data*; EC02TV-CA; U. S. Census Bureau: Washington, DC, 2002; http://www.census.gov/svsd/www/02vehinv.html.
(26) Hinds, W. C. Aerosol technology: Properties, behavior, and measurement of airborne particles, 2nd ed.; Wiley: New York, 1982.
(27) Misra, C.; Kim, S.; Shen, S.; Sioutas, C. A high flow rate, very low-pressure drop impactor for inertial separation of ultrafine from accumulation mode particles. *J. Aerosol Sci.* **2002**, *33*, 735−752.
(28) Dzubay, T. G. *X-ray Analysis of Environmental Samples*; Ann Arbor Science Publishing: Ann Arbor, MI, 1977.
(29) Birch, M. E.; Cary, R. A. Elemental carbon-based method for monitoring occupational exposures to particulate diesel exhaust. *Aerosol Sci. Technol.* **1996**, *25*, 221−241.
(30) Muller, P. K.; Mendoza, B. V.; Collins, J. C.; Wilgus, E. A. *Ion Chromatography Analysis of Environmental Pollutants*; Ann Arbor Science Publishing: Ann Arbor, MI, 1977.
(31) Mader, B. T.; Pankow, J. F. Gas/solid partitioning of semivolatile organic compounds (SOCs) to air filters. 3. An analysis of gas adsorption artifacts in measurements of atmospheric SOCs and organic carbon (OC) when using Teflon membrane filters and quartz fiber filters. *Environ. Sci. Technol.* **2001**, *35*, 3422−3432.
(32) Abdul-Khalek, I. S.; Kittelson, D. B.; Graskow, B. R.; Wei, Q.; Brear, F. *Diesel Exhaust Particle Size: Measurement Issues and Trends*; SAE Paper 980525; SAE International: Warrendale, PA, 1998.
(33) Abu-Allaban, M.; Coulomb, W.; Gertler, A. W.; Gillies, J.; Pierson, W. R.; Rogers, C. F.; Sagebiel, J. C.; Tarnay, L. Exhaust particle size distribution measurements at the Tuscarora Mountain tunnel. *Aerosol Sci. Technol.* **2002**, *36*, 771−789.
(34) Kittelson, D. B. Engines and nanoparticles: A review. *J. Aerosol Sci.* **1998**, *29*, 575−588.
(35) Ristovski, Z. D.; Jayaratne, E. R.; Lim, M.; Ayoko, G. A.; Morawska, L. Influence of the fuel sulfur content on the particulate emissions from a bus city fleet. In *Proceedings of the 16th International Clean Air and Environment Conference of the Clean Air Society of Australia and New Zealand*, Sydney, Australia, Aug 19−22, 2002; CASANZ: New South Wales, Australia, 2002.
(36) CONCAWE. *Measurements of the Number and Mass Weighted Size Distributions of Exhaust Particles Emitted from European Heavy Duty Engines*; Report 01/51; CONCAWE: Brussels, Belgium, 2001.
(37) Morawska, L.; Zhang, J. F. Combustion sources of particles. 1. Health relevance and source signatures. *Chemosphere* **2002**, *49*, 1045−1058.
(38) Jamriska, M.; Morawska, L.; Thomas, S.; He, C. Diesel bus emissions measured in a tunnel study. *Environ. Sci. Technol.* **2004**, *38*, 6701−6709.
(39) Kittelson, D. B.; Johnson, J.; Watts, W.; Wei, Q.; Dryton, M.; Paulson, D.; Bukowiecki, N. *Diesel Aerosol Sampling in the Atmosphere, Government/Industry Meeting*; SAE Technical Paper Series 2000-01-2212; SAE International: Washington, DC, 2000.
(40) Gidhagen, L.; Johansson, C.; Strom, J.; Kristensson, A.; Swietlicki, E.; Pirjola, L.; Hansson, H. C. Model simulation of ultrafine particles inside a road tunnel. *Atmos. Environ.* **2003**, *37*, 2023−2036.
(41) Kristensson, A.; Johansson, C.; Westerholm, R.; Swietlicki, E.; Gidhagen, L.; Wideqvist, U.; Vesely, V. Real-world traffic emission factors of gases and particles measured in a road tunnel in Stockholm, Sweden. *Atmos. Environ.* **2004**, *38*, 657−673.
(42) Maricq, M. M.; Podsiadlik, D. H.; Chase, R. E. Gasoline vehicle particle size distributions: Comparison of steady state, FTP, and US06 measurements. *Environ. Sci. Technol.* **1999**, *33*, 2007−2015.
(43) Maricq, M. M.; Podsiadlik, D. H.; Chase, R. E. Examination of the size-resolved and transient nature of motor vehicle particle emissions. *Environ. Sci. Technol.* **1999**, *33*, 1618−1626.
(44) Hughes, L. S.; Allen, J. O.; Salmon, L. G.; Mayo, P. R.; Johnson, R. J.; Cass, G. R. Evolution of nitrogen species air pollutants along trajectories crossing the Los Angeles area. *Environ. Sci. Technol.* **2002**, *36*, 3928−3935.
(45) Mader, B. T.; Schauer, J. J.; Seinfeld, J. H.; Flagan, R. C.; Yu, J. Z.; Yang, H.; Lim, H. J.; Turpin, B. J.; Deminter, J. T.; Heidemann, G.; Bae, M. S.; Quinn, P.; Bates, T.; Eatough, D. J.; Huebert, B. J.; Bertram, T.; Howell, S. Sampling methods used for the collection of particle-phase organic and elemental carbon during ACE−Asia. *Atmos. Environ.* **2003**, *37*, 1435−1449.
(46) Schauer, C.; Niessner, R.; Poschl, U. Polycyclic aromatic hydrocarbons in urban air particulate matter: Decadal and seasonal trends, chemical degradation, and sampling artifacts. *Environ. Sci. Technol.* **2003**, *37*, 2861−2868.
(47) Claiborn, C.; Pang, Y.; Finn, D.; Gundel, L.; Larson, T.; Liu, S. The fine particulate organic carbon measurement artifact and its implications for exposure assessment. *Epidemiology* **2002**, *13*, S238−S238.
(48) Kowalczyk, G. S.; Gordon, G. E.; Rheingrover, S. W. Identification of atmospheric particulate sources in Washington, DC, using chemical−element balances. *Environ. Sci. Technol.* **1982**, *16*, 79−90.
(49) Gertler, A. W.; Gillies, J. A.; Pierson, W. R. An assessment of the mobile source contribution to PM10 and PM2.5 in the United States. *Water, Air, Soil Pollut.* **2000**, *123*, 203−214.
(50) Wrobel, A.; Rokita, E.; Maenhaut, W. Transport of traffic-related aerosols in urban areas. *Sci. Total Environ.* **2000**, *257*, 199−211.
(51) Pakkanen, T. A.; Loukkola, K.; Korhonen, C. H.; Aurela, M.; Makela, T.; Hillamo, R. E.; Aarnio, P.; Koskentalo, T.; Kousa, A.; Maenhaut, W. Sources and chemical composition of atmospheric fine and coarse particles in the Helsinki area. *Atmos. Environ.* **2001**, *35*, 5381−5391.
(52) Zielinska, B.; Sagebiel, J.; McDonald, J. D.; Whitney, K.; Lawson, D. R. Emission rates and comparative chemical composition from selected in-use diesel and gasoline-fueled vehicles. *J. Air Waste Manage. Assoc.* **2004**, *54*, 1138−1150.
(53) McDonald, J. D.; Barr, E. B.; White, R. K.; Chow, J. C.; Schauer, J. J.; Zielinska, B.; Grosjean, E. Generation and characterization of four dilutions of diesel engine exhaust for a suhchronic inhalation study. *Environ. Sci. Technol.* **2004**, *38*, 2513−2522.
(54) Smith, K. R.; Aust, A. E. Mobilization of iron from urban particulates leads to generation of reactive oxygen species in vitro and induction of ferritin synthesis in human lung epithelial cells. *Chem. Res. Toxicol.* **1997**, *10*, 828−834.
(55) Lighty, J. S.; Veranth, J. M.; Sarofim, A. F. Combustion aerosols: Factors governing their size and composition and implications to human health. *J. Air Waste Manage. Assoc.* **2000**, *50*, 1565−1618.
(56) Sanders, P. G.; Xu, N.; Dalka, T. M.; Maricq, M. M. Airborne brake wear debris: Size distributions, composition, and a comparison of dynamometer and vehicle tests. *Environ. Sci. Technol.* **2003**, *37*, 4060−4069.

(57) Singh, M.; Jaques, P. A.; Sioutas, C. Size distribution and diurnal characteristics of particle-bound metals in source and receptor sites of the Los Angeles Basin. *Atmos. Environ.* **2002**, *36*, 1675−1689.
(58) Clarke, A. G.; Chen, J. M.; Pipitsangchand, S.; Azadi Bougar, G. A. Vehicular particulate emissions and roadside air pollution. *Sci. Total Environ.* **1996**, *190*, 417−422.
(59) Hildemann, L. M.; Markowski, G. R.; Cass, G. R. Chemical-composition of emissions from urban sources of fine organic aerosol. *Environ. Sci. Technol.* **1991**, *25*, 744−759.
(60) Schauer, J. J.; Cass, G. R. Source apportionment of wintertime gas-phase and particle-phase air pollutants using organic compounds as tracers. *Environ. Sci. Technol.* **2000**, *34*, 1821−1832.
(61) Garg, B. D.; Cadle, S. H.; Mulawa, P. A.; Groblicki, P. J.; Laroo, C.; Parr, G. A. Brake wear particulate matter emissions. *Environ. Sci. Technol.* **2000**, *34*, 4463−4469.
(62) Sardar, S. B.; Fine, P. M.; Sioutas, C. Seasonal and spatial variability of the size-resolved chemical composition of particulate matter (PM10) in the Los Angeles Basin. *J. Geophys. Res., [Atmos.]* **2005**, *110* (D7), http://dx.doi.org/10.1029/2004JD004627.
(63) Sternbeck, J.; Sjodin, A.; Andreasson, K. Metal emissions from road traffic and the influence of resuspension—Results from two tunnel studies. *Atmos. Environ.* **2002**, *36*, 4735−4744.
(64) Harrison, R. M.; Tilling, R.; Romero, M. S. C.; Harrad, S.; Jarvis, K. A study of trace metals and polycyclic aromatic hydrocarbons in the roadside environment. *Atmos. Environ.* **2003**, *37*, 2391−2402.
(65) Park, K.; Kittelson, D. B.; Zachariah, M. R.; McMurry, P. H. Measurement of inherent material density of nanoparticle agglomerates. *J. Nanopart. Res.* **2004**, *6*, 267−272.
(66) Abu-Allaban, M.; Gillies, J. A.; Gertler, A. W.; Clayton, R.; Proffitt, D. Tailpipe, resuspended road dust, and brake-wear emission factors from on-road vehicles. *Atmos. Environ.* **2003**, *37*, 5283−5293.
(67) Li, N.; Alam, J.; Venkatesan, M. I.; Eiguren-Fernandez, A.; Schmitz, D.; Di Stefano, E.; Slaughter, N.; Killeen, E.; Wang, X. R.; Huang, A.; Wang, M. Y.; Miguel, A. H.; Cho, A.; Sioutas, C.; Nel, A. E. Nrf2 is a key transcription factor that regulates antioxidant defense in macrophages and epithelial cells: Protecting against the proinflammatory and oxidizing effects of diesel exhaust chemicals. *J. Immunol.* **2004**, *173*, 3467−3481.
(68) Harris, S. J.; Maricq, M. M. Signature size distributions for diesel and gasoline engine exhaust particulate matter. *J. Aerosol Sci.* **2001**, *32*, 749−764.
(69) Sakurai, H.; Tobias, H. J.; Park, K.; Zarling, D.; Docherty, S.; Kittelson, D. B.; McMurry, P. H.; Ziemann, P. J. On-line measurements of diesel nanoparticle composition and volatility. *Atmos. Environ.* **2003**, *37*, 1199−1210.
(70) Bagley, S. T.; Gratz, L. D.; Johnson, J. H.; McDonald, J. F. Effects of an oxidation catalytic converter and a biodiesel fuel on the chemical, mutagenic, and particle size characteristics of emissions from a diesel engine. *Environ. Sci. Technol.* **1998**, *32*, 1183−1191.
(71) Holmen, B. A.; Ayala, A. Ultrafine PM emissions from natural gas, oxidation-catalyst diesel, and particle-trap diesel heavy-duty transit buses. *Environ. Sci. Technol.* **2002**, *36*, 5041−5050.

Received for review February 22, 2005. Revised manuscript received June 30, 2005. Accepted September 13, 2005.

ES050360S